

Ultrasound directed self-assembly processing of nanocomposite materials with ultra-high carbon nanotube weight fraction

J Greenhall, L Homel and B Raeymaekers 

Abstract

We introduce a new process to manufacture polymer nanocomposite materials reinforced with an ultra-high weight fraction of aligned carbon nanotubes. This process is based on using ultrasound directed self-assembly, which employs the force associated with a standing ultrasound wave to concentrate and align carbon nanotubes dispersed in the polymer matrix. In contrast with existing manufacturing processes, which typically limit the carbon nanotube weight fraction to approximately 1 wt.%, we demonstrate manufacturing polymer nanocomposite materials with more than 10 wt.% of aligned carbon nanotubes along a single line. We accomplish this by first dispersing 1 wt.% percent of carbon nanotubes in the polymer matrix, and using ultrasound directed self-assembly to concentrate and align the carbon nanotubes along a single line. Then, we trim the excess material around the single line of aligned carbon nanotubes to retain a nanocomposite material with an ultra-high weight percent of aligned carbon nanotubes. We also manufacture polymer nanocomposite materials with different weight percent of aligned carbon nanotubes along multiple parallel lines, and with randomly oriented carbon nanotubes. We experimentally measure the mechanical properties of the polymer nanocomposite materials, and find that the ultrasound directed self-assembly process results in specimens with aligned carbon nanotubes that display a significant increase in ultimate tensile strength, Young's modulus, and moduli of resilience and toughness, compared to benchmark materials including polymer nanocomposite materials with randomly oriented carbon nanotubes, and virgin polymer matrix material.

Keywords

Ultrasound, directed self-assembly, materials, polymer, nanocomposites

Introduction

Polymer nanocomposite materials consist of a polymer matrix reinforced with a nanoscale filler material, and are of interest to the scientific community because of their unique physical properties.¹ In particular, polymer nanocomposite materials reinforced with carbon nanotubes (CNTs) have received considerable attention due to their potential as ultra-strong, lightweight materials, displaying a tensile strength and Young's modulus as high as 3.6 GPa and 80 GPa, respectively.² To achieve these exotic properties, four critical aspects must be addressed: (1) CNT dispersion in the polymer matrix material,³ (2) adhesion between the matrix material and CNTs,⁴ (3) CNT weight fraction within the nanocomposite material,^{5,6} and (4) alignment of the CNTs parallel to the direction of the external

mechanical load.⁷ This work focuses on aligning an ultra-high weight fraction of CNTs (> 10%) in the polymer matrix material.

Techniques for aligning CNTs in a polymer material may be categorized as (1) methods that extrude and spin a thin fiber with aligned CNTs that is subsequently embedded in a polymer matrix, and (2) methods that align CNTs directly in the polymer matrix. Several researchers have employed extrusion and spinning

Department of Mechanical Engineering, University of Utah, USA

Corresponding author:

B Raeymaekers, University of Utah, 1495 East 100 South, MEK 1550, Salt Lake City, UT 84112, USA.
 Email: bart.raeymaekers@utah.edu

techniques to produce a thin continuous fiber with bundles of aligned CNTs.^{8,9} These methods produce fibers with a diameter on the order of tens of micrometers and display high tensile strength due to a large weight fraction of CNTs aligned parallel to the fiber axis. However, the fibers require significant post-processing to achieve the final geometry of the polymer nanocomposite material. In contrast, aligning CNTs directly in the matrix material does not require post-processing, but creates discontinuous reinforcement of the polymer matrix, which results in a material of lower strength, compared to materials with continuous reinforcement. Several techniques for aligning CNTs in a polymer material have been documented in the literature, including mechanical stretching,¹⁰ cutting,¹¹ shear flow,¹² and external field-based techniques employing electric,^{13,14} magnetic,¹⁵ or ultrasound fields.^{16–18} Stretching, cutting, and shear flow techniques align CNTs by applying mechanical stress to the polymer material. However, the alignment processes limit the polymer nanocomposite material geometry to thin films (e.g. <200 nm for Ajayan et al.¹¹) or significantly deform the material (up to 330% elongation for Jin et al.¹⁰). Alternatively, external fields align CNTs without constraining the geometry of the final polymer nanocomposite material specimen. When exposed to electric or magnetic fields, CNTs align either parallel or perpendicular to the direction of the applied field, depending on their electric and magnetic properties,^{13,15} which in turn depend on the CNT growth method.¹⁹ However, electric and magnetic field techniques require extremely high field strengths (20.0 kV/m and 80.0 kOe, for Kamat et al.¹⁴ and Fujiwara et al.,¹⁵ respectively) and, thus, they do not easily scale to cover large areas or volumes, which limit the viability of these methods to manufacture macroscale polymer nanocomposite specimens. Alternatively, ultrasound directed self-assembly allows organizing patterns of aligned CNTs using the acoustic radiation force associated with a standing ultrasound wave. This technique works independent of the CNT material properties,²⁰ and weak attenuation of ultrasound waves in most low-viscosity liquids²¹ reduces the need for ultra-high field strengths. Saito et al.²² showed that a polymer composite material can be fabricated by solidifying a particle suspension consisting of spheres or rods in polysiloxane resin, organized into a line-pattern using a standing ultrasound wave, but they did not quantify the mechanical properties of the fabricated materials. Furthermore, Scholz et al.²³ used ultrasound standing waves to manufacture thin, single layers of short glass fiber-reinforced polymer composite materials, and showed a 43% increase of fracture strength in the direction of the fiber reinforcement. Haslam and Raeymaekers¹⁷ used standing ultrasound waves to

align CNTs into multiple discontinuous fibers, and documented that the ultimate tensile strength and Young's modulus increase with increasing CNT weight fraction.¹⁷

To obtain polymer nanocomposite materials with ultra-high strength and stiffness, we align an ultra-high weight fraction of CNTs within a liquid urethane resin, which is then cured to form a polymer matrix containing CNTs aligned parallel to the anticipated external mechanical load. However, increasing the CNT weight fraction increases the viscosity of the CNT/resin mixture,²⁴ increases CNT entanglement and clustering, and decreases dispersion and alignment of the CNTs within the resin.⁵ Few publications exist in the open literature that document alignment of an ultra-high CNT weight fraction in a polymer matrix. Hence, the objective of this work is to experimentally demonstrate a process for manufacturing polymer nanocomposite materials reinforced with aligned CNTs with a weight fraction in excess of 10 wt.%. We manufacture specimens with different weight percent of randomly oriented and aligned CNTs along a single line or multiple parallel lines. We quantify the ultimate tensile strength, Young's modulus, and moduli of resilience and toughness of these materials as a function of the CNT weight fraction and alignment.

Materials and methods

Ultrasound directed self-assembly enables manipulating single particles,²⁵ creating patterns of multiple particles,^{26,27} and aligning particles¹⁷ dispersed in a fluid medium, using the acoustic radiation force associated with a standing ultrasound wave. The acoustic radiation force acting on a spherical particle with radius R , in an inviscid fluid medium, and subject to a plane ultrasound standing wave with wavelength $\lambda_0 \gg R$ and harmonic pressure $p = p_0 \sin(k_0 x)$, is given as²⁰

$$F = \frac{\pi R^3}{3} p_0^2 k_0 \beta_m \Phi \sin(2k_0 x) \quad (1)$$

Here, p_0 is the pressure amplitude of the standing ultrasound wave with wave number $k_0 = 2\pi/\lambda_0$, $\Phi = (5\rho_p - 2\rho_m)/(2\rho_p + \rho_m) - \beta_p/\beta_m$ is the acoustic contrast factor, and the subscripts m and p refer to the fluid medium and particle, respectively, with density ρ , sound propagation velocity c , and compressibility $\beta = 1/\rho c^2$. x is the distance from the ultrasound source. Equation (1) shows that the sign of the acoustic contrast factor determines whether the acoustic radiation force drives the particle towards the nodes ($\Phi > 0$) or the antinodes ($\Phi < 0$) of the standing ultrasound wave. In this work, we will only consider an

acoustic contrast factor $\Phi > 0$, which is the case of CNTs in liquid urethane resin. Researchers have extended the acoustic radiation force theory to include viscous terms, showing that the amplitude of the acoustic radiation force decreases in a viscous medium, but that the positions where particles assemble are identical in viscous and inviscid media.²⁸ Additionally, the acoustic radiation force theory has been extended to cylindrical particles (e.g. CNTs), demonstrating that the acoustic radiation force drives the cylindrical particles to and aligns them with the nodes of the standing ultrasound wave.²⁹ Thus, ultrasound directed self-assembly enables aligning CNTs in a liquid urethane resin, by designing a standing ultrasound wave for which the nodes coincide with the desired CNT locations and alignment. It is important to note that the magnitude of the acoustic radiation force and viscous drag force that drive the CNT motion is dependent on the particle size and the ultrasound standing wave frequency, and limits the rate at which the particles can be organized at the nodes of the ultrasound standing wave.²⁶ As a result, short polymer resin curing times constrain the smallest particle size and/or lowest frequency that can successfully organize and align the particles at the nodes of the ultrasound standing wave. The particle size limit is also dependent on the material properties of the particles and the matrix material, i.e., the diffusion coefficient increases with decreasing particle size and increasing time needed to displace the particle from its initial position to the node of the ultrasound standing wave, which renders the effect of Brownian motion increasingly important.

Figure 1 shows a schematic of the experimental set-up to manufacture macroscale dogbone polymer nanocomposite specimens. It consists of a high-density polyethylene dogbone-shaped reservoir with a gauge section of length $L = 16$ mm and width $W = 3.65$ mm (ASTM

D638³⁰), which contains a liquid urethane resin with dispersed CNTs. Two recess slots in the gauge section position two parallel, opposing piezoelectric ultrasound transducers (PZT-4, 190 kHz center frequency), separated by W , and driven by a function generator (Tektronix AFG3102) and a radio frequency power amplifier (E&I 440LA), to enable ultrasound directed self-assembly and alignment of CNTs in the gauge section of the dogbone reservoir. The bottom of the reservoir consists of a glass plate coated with an anti-adhesion layer that facilitates evacuating the specimen, after the liquid urethane resin polymerizes. We apply a sinusoidal voltage with frequency f to the ultrasound transducers to perform ultrasound directed self-assembly in the gauge section of the dogbone reservoir, which creates a standing ultrasound wave with $N = 2Wf/c_m$ nodes in the liquid urethane resin, where c_m is the sound propagation velocity in the urethane resin. To align a CNT weight fraction in excess of 10 wt.%, we first disperse a small weight fraction (≤ 1 wt.%) of CNTs in the liquid urethane resin, and then employ ultrasound directed self-assembly to concentrate and align the CNTs along a single line in the center of the gauge section of the reservoir. We ensure that there is exactly one line of aligned CNTs in the middle of the gauge section of the reservoir ($N = 1$) by adjusting the operating frequency of the ultrasound transducers, such that the wavelength of the standing ultrasound wave $\lambda_0 = 2W$.

Figure 2 schematically illustrates the process of manufacturing macroscale dogbone polymer nanocomposite specimens with an ultra-high weight fraction of aligned CNTs. We use a two-part thermoset urethane resin (Smooth-Cast 300, Smooth-On, Inc.) with a viscosity of 80 cps at 25°C in its liquid state, a density of 1.05 g/cm³, a pot life of 3 min,³¹ and a sound propagation velocity $c_m = 1400$ m/s (based on a pulse-echo measurement). We select this low-viscosity urethane resin to minimize the effect of viscous attenuation of the standing ultrasound wave within the reservoir, which facilitates ultrasound directed self-assembly.²⁸ We use commercially available multi-walled CNTs (MWCNTs) of length 10–20 µm and diameter of 50–80 nm, fabricated using chemical vapor deposition (95% pure). This results in a ratio of MWCNT diameter to wavelength of the standing ultrasound wave between 6.78×10^{-6} and 10.85×10^{-6} . We dry the MWCNTs on a furnace at 65°C before mixing them in Part A of the liquid urethane resin (Figure 2(a)). Next, we disperse the CNTs in Part A of the liquid urethane resin by introducing the anionic surfactant sodium dodecylbenzenesulfonate (NaDDBS – Tokyo Chemical Industry Co., LTD) that reduces the van der Waals attraction between adjacent MWCNTs,^{32,33} and applying tip sonication (Hielscher UP50H) to physically separate adjacent MWCNTs³⁴ (Figure

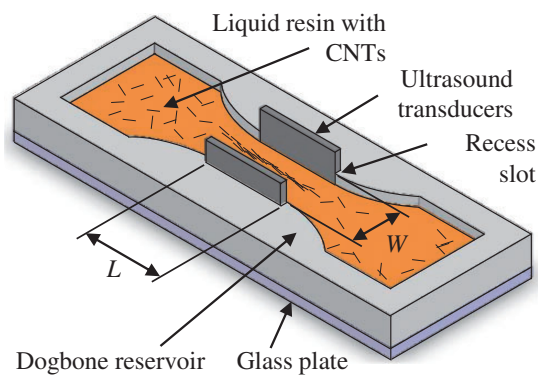


Figure 1. Schematic of the experimental set-up to manufacture macroscale dogbone specimens of polymer nanocomposite material with aligned carbon nanotubes (CNTs) (not drawn to scale).

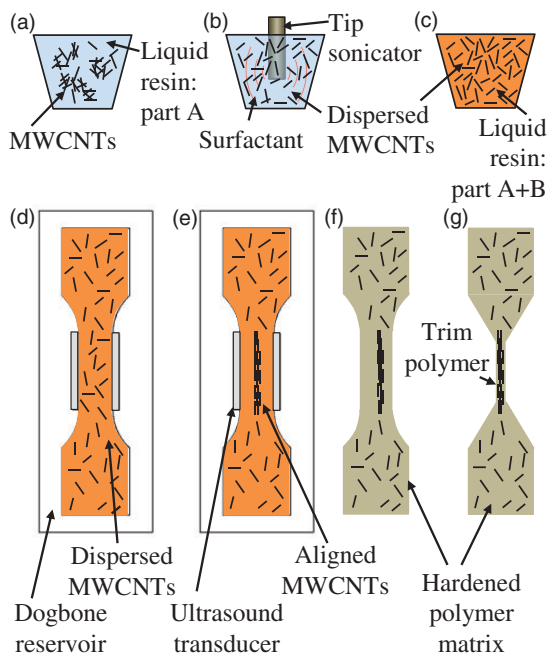


Figure 2. Schematic of the manufacturing process of macro-scale dogbone specimens of polymer nanocomposite material with aligned multi-walled carbon nanotubes (MWCNTs) (not drawn to scale).

2(b)). Based on prior experiments in our lab with 0.1–0.5 wt.% MWCNTs, dispersion is best achieved using a surfactant to MWCNT weight ratio of 6:10. We add Part B of the liquid urethane resin, which initiates polymerization of the liquid urethane resin (Figure 2(c)), and then cast the mixture in the dogbone reservoir (Figure 2(d)). We subsequently perform ultrasound directed self-assembly by energizing the two opposing ultrasound transducers, which generate a standing ultrasound wave that concentrates and aligns the MWCNTs along a single line at the center of the gauge section of the dogbone reservoir (Figure 2(e)). We continue to energize the ultrasound transducers until the liquid urethane resin polymerizes and the aligned MWCNTs are fixated in place. We evacuate the polymerized dogbone specimen from the reservoir (Figure 2(f)), and trim the polymer matrix from the dogbone gauge section so that we retain only the single line that contains an ultra-high weight percent of aligned MWCNTs (Figure 2(g)). This manufacturing process contrasts existing work,¹⁷ where MWCNTs are aligned along multiple lines in the gauge section of the dogbone specimen and the entire gauge section is left intact.

We quantify the ultimate tensile strength, Young's modulus, and moduli of resilience and toughness of the dogbone nanocomposite specimen, from a stress-strain curve obtained using uniaxial tensile testing with a strain rate of 2 mm/min (Instron 4303/MTS model

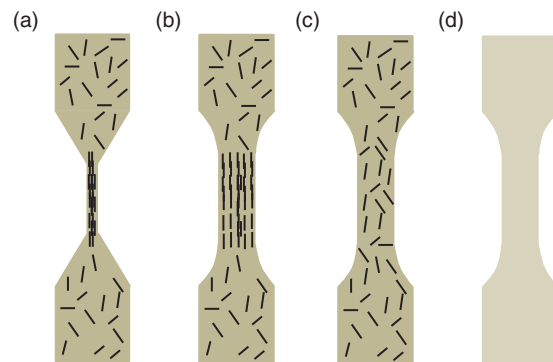


Figure 3. Dogbone specimens consisting of (a) the polymer nanocomposite material reinforced with a single line of aligned multi-walled carbon nanotubes (MWCNTs), and benchmark materials including (b) polymer matrix with multiple ($N = 16$) lines of aligned MWCNTs, (c) polymer matrix with randomly oriented MWCNTs, and (d) virgin polymer matrix.

632.26) following the ASTM D638 standard test method for tensile properties of plastics.³⁰ Specifically, we determine the Young's modulus from the slope in the proportional region of stress–strain curve, whereas the moduli of resilience and toughness result from the integral under the stress–strain curve up to the yield and fracture strain, respectively. To evaluate the effect of MWCNT reinforcement on the mechanical properties of the polymer nanocomposite materials, we compare the tensile properties to those of benchmark materials. Figure 3 illustrates (a) the polymer nanocomposite dogbone specimen consisting of polymer matrix reinforced with a single line of aligned MWCNTs, and the benchmark material dogbone specimens, consisting of (b) polymer matrix with multiple ($N = 16$) lines of aligned MWCNTs, similar to the work presented in Haslam and Raeymaekers,¹⁷ (c) polymer matrix with randomly oriented MWCNTs, and (d) virgin polymer matrix. We manufacture these specimens with a similar process as the one shown in Figure 2, but increase the operating frequency of the ultrasound transducers and do not trim the material after curing when manufacturing the specimens of Figure 3(b). Additionally, we only disperse but not align the MWCNTs to manufacture the specimens of Figure 3(c).

We manufacture dogbone specimens containing a single line of aligned MWCNTs (Figure 3(a)) using a weight fraction of approximately 11 wt.% with a standard deviation of 2 wt.%. To calculate the weight fraction of MWCNTs for this specimen type, we first remove the polymer material around the single line of aligned MWCNTs by sanding. Then, we determine the density of the polymer nanocomposite material specimen ρ_c using Archimedes' method, measuring its weight in air and in water, i.e. $\rho_c = \rho_w m_c / (m_c - m'_c)$, where ρ_w is the density of water, m_c is the measured weight of the polymer

nanocomposite material in air, and m_c^w is the measured weight of the polymer nanocomposite material submerged in water. We then use the rule of mixtures with the density of the polymer matrix $\rho_{poly} = 1.05 \text{ g/cm}^3$ ³¹ and the MWCNTs $\rho_{MWCNT} = 0.18 \text{ g/cm}^3$ ³⁵ to determine the volume fraction of MWCNTs, $v = (\rho_c - \rho_{poly}) / (\rho_{MWCNT} - \rho_{poly})$, which is used to compute the weight fraction as $w = v \rho_{MWCNT} / m_c$. Alternatively, we manufacture the benchmark dogbone specimens containing multiple lines of MWCNTs (Figure 3(b)) and randomly oriented MWCNTs (Figure 3(c)) using a weight fraction between 0.1 and 10.0 wt.%, measured by weighing the polymer matrix and MWCNTs before they are dispersed and cast into the dogbone reservoir. We have manufactured all dogbone specimens that contain MWCNTs (Figure 3(a) to (c)) using a constant surfactant to MWCNT weight ratio of 6:10. Additionally, we have exposed all dogbone specimens (Figure 3(a) to (d)) to the same ultrasound energy.

Results and discussion

Figure 4 shows the ultimate tensile strength σ_{UT} , as a function of the MWCNT weight fraction w , for the polymer nanocomposite material with a single line of aligned MWCNTs and the benchmark materials. Each data point represents an average ultimate tensile strength of between 5 and 12 specimens, and the error bars represent the standard deviation of the ultimate tensile strength measurements. From Figure 4 we observe that σ_{UT} of the nanocomposite materials with a weight fraction of randomly oriented MWCNTs (diamond marker) (<2.5 wt.%) is approximately 40% higher than the ultimate tensile strength of the virgin polymer material. However, increasing the weight

fraction of randomly oriented MWCNTs in excess of 2.5 wt.% decreases σ_{UT} . This is due to increased MWCNT entanglement and clustering with increasing weight fraction of MWCNTs, which inhibits dispersion and prevents load transfer from the polymer matrix to the MWCNTs.⁵ Alternatively, we observe that aligning the MWCNTs along multiple lines (triangle marker) increases σ_{UT} compared to that of specimens with randomly oriented MWCNTs of the same MWCNT weight fraction. Aligning the MWCNTs in the direction of the external mechanical load enables transferring a greater fraction of that load from the polymer matrix to the MWCNTs,¹⁷ and it also inhibits MWCNT entanglement and clustering.^{2,5} However, for specimens containing multiple lines of aligned MWCNTs, we still observe decreasing σ_{UT} with increasing MWCNT weight fraction in excess of 2.5 wt.%. During the manufacturing process, we mix a high weight fraction of MWCNTs in the liquid urethane resin, which impedes dispersion,³⁴ and increases the viscosity of the MWCNT/resin mixture,²⁴ thus obstructing alignment of the MWCNTs through ultrasound directed self-assembly. Finally, we observe that the polymer nanocomposite materials containing a single line of aligned MWCNTs (square marker) display a significantly higher σ_{UT} than that of the benchmark materials, which is in agreement with trends reported in the literature.^{2,5,17} In contrast with the benchmark materials, which suffer from limited MWCNT dispersion for high MWCNT weight fractions, the polymer nanocomposite materials containing a single line of aligned MWCNTs achieve good MWCNT dispersion because during the manufacturing process, dispersion is performed within liquid urethane resin containing a low weight fraction (<1.0 wt.%) of MWCNTs. Subsequently, ultrasound directed self-assembly concentrates and aligns the MWCNTs along a single line, creating a locally high weight fraction of MWCNTs (>10 wt.%).

Figure 5 shows the Young's modulus E as a function of MWCNT weight fraction, for the polymer nanocomposite material with a single line of aligned MWCNTs and the benchmark materials. Each data point represents an average of between 5 and 12 measurements, and the error bars represent the standard deviation of all measurements for each data point. From Figure 5, we observe that adding even a small weight fraction (<1 wt.%) of randomly oriented MWCNTs to the polymer matrix (diamond marker) increases E by more than 100 % compared to E_{poly} of the virgin polymer matrix. However, similarly to σ_{UT} , increasing the weight fraction of randomly oriented MWCNTs decreases E due to clustering and entanglement of the MWCNTs. Alternatively, we observe that multiple lines of aligned MWCNTs (triangle marker) increase E with increasing MWCNT weight fraction. We observe a similar trend

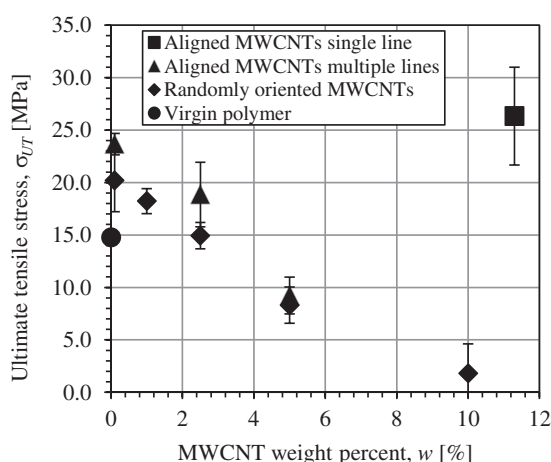


Figure 4. Ultimate tensile strength versus multi-walled carbon nanotube (MWCNT) weight fraction.

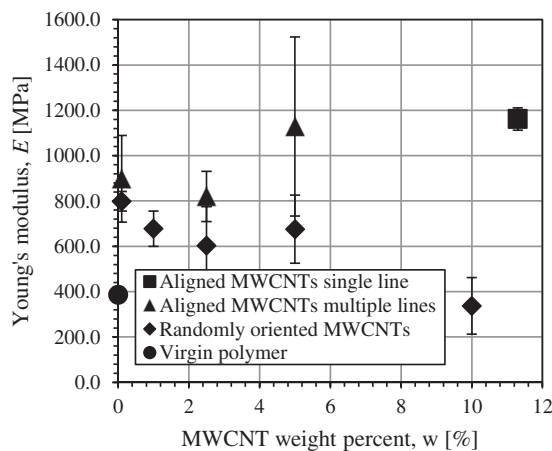


Figure 5. Young's modulus versus multi-walled carbon nanotube (MWCNT) weight fraction.

for the specimens containing a single line of aligned MWCNTs (square marker), for which the average value of E is larger than all benchmark materials. This can be explained by the axial stiffness of the MWCNTs,¹⁹ and the rule of mixtures, which shows that as the weight fraction of MWCNTs increases, the stiffness of the polymer nanocomposite material approaches that of the MWCNTs.⁷ However, the polymer nanocomposite material only benefits from the exotic axial stiffness properties of the MWCNTs if they are aligned in the direction of the external mechanical load. Adding MWCNTs to the polymer matrix results in a more significant increase in the Young's modulus than in the ultimate tensile strength of the polymer nanocomposite material, shown in Figure 4, which is in agreement with other results documented in the literature.^{2,4,17}

Figure 6 shows (a) the modulus of resilience U_R and (b) the modulus of toughness U_T as a function of MWCNT weight fraction, for the polymer nanocomposite material containing a single line of aligned MWCNTs and the benchmark materials. Each data point represents an average of between 5 and 12 measurements, and the error bars represent the standard deviation of all measurements for each data point. From Figure 6(a), we observe that for an MWCNT weight fraction of less than 1.0 wt.%, the benchmark materials containing randomly oriented MWCNTs (diamond marker) and multiple lines of aligned MWCNTs (triangle marker) display U_R values that are 60% and 40% larger, respectively, than that of the virgin polymer matrix. However, increasing the MWCNT weight fraction beyond 1.0 wt.% decreases U_R because MWCNT clustering and entanglement lower the yield strength of the benchmark specimens, similarly to σ_{UT} shown in Figure 4, without significantly lowering the Young's modulus of the benchmark

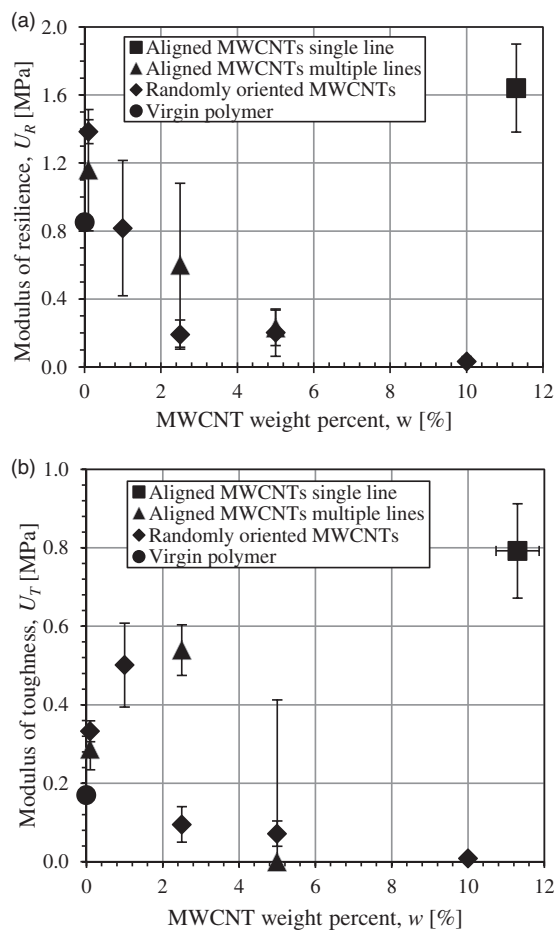


Figure 6. (a) Modulus of resilience and (b) modulus of toughness versus multi-walled carbon nanotube (MWCNT) weight fraction.

specimens. As a result, the low yield strength and high Young's modulus benchmark specimens are susceptible to plastic deformation even under small loads, as indicated by the small U_R values. Similarly, from Figure 6(b), we observe that an MWCNT weight fraction in excess of 2.5 wt.% drastically reduces U_T of the benchmark specimens containing randomly oriented MWCNTs (diamond marker) and multiple lines of aligned MWCNTs (triangle marker). Obtaining well-dispersed MWCNTs in the liquid urethane resin is challenging for such high weight fractions, and the resulting polymer nanocomposite materials become brittle and susceptible to fracture under a small external mechanical load. Physically, this occurs due to stress concentrations in the vicinity of large clusters of undispersed MWCNTs, which initiate crack growth under small external mechanical load.⁵ In contrast, we observe from Figure 6(a) and (b) that the specimens containing a single line of aligned MWCNTs (square marker) achieve U_R and U_T values that are approximately 200% and 450% larger, respectively, than those of

the virgin polymer. These increases result from transferring the external mechanical loading from the polymer matrix material to the well-dispersed aligned MWCNTs, which enable the polymer nanocomposite material to withstand a higher external mechanical load before yielding or failing. These results indicate that the new manufacturing process documented in this work enables obtaining an ultra-high weight fraction of well-dispersed MWCNTs aligned parallel to the external mechanical load, which results in a significant increase in the moduli of resilience and toughness.

The results demonstrate that reinforcing polymer nanocomposite materials with an ultra-high weight fraction (>10 wt.%) of aligned MWCNTs increases the ultimate tensile strength, Young's modulus, and moduli of resilience and toughness. However, dispersion is a significant challenge with increasing MWCNT weight fraction. In this work, we use an identical process to disperse MWCNTs in the liquid urethane resin, irrespective of the weight fraction, and we perform no specific analysis to quantify how well the MWCNTs are dispersed. The size of the error bars in Figures 4 to 6 reveals that repeatability of the experiments decreases with increasing MWCNT weight fraction, suggesting decreasing dispersion. This is substantiated by visual inspection of the dogbone specimen fracture surfaces after tensile testing, where we typically observe a higher number of MWCNT clusters in the benchmark material specimens containing a large weight fraction of either multiple lines of aligned MWCNTs or randomly oriented MWCNTs. Conversely, the new manufacturing process demonstrated in this work circumvents the dispersion problem by performing dispersion for a low weight fraction of MWCNTs, and then using ultrasound directed self-assembly to concentrate and align the MWCNTs along a single line with locally high weight fraction. As a result, the error bars are smaller than for the nanocomposite materials with multiple lines of aligned MWCNTs. We point out that all stress-strain curves from which the results of Figures 4 to 6 are extracted, show almost linear behavior until fracture, i.e. little plasticity is observed. We also note that Figures 4 to 6 do not offer a direct comparison between material specimens with a single and multiple lines of MWCNTs of the same weight percent. Indeed, manufacturing specimens with a single line of low weight percent MWCNTs renders it difficult to extract the single line from the polymer matrix and quantify its weight percent and mechanical properties in a repeatable fashion. Manufacturing specimens with multiple lines of high weight percent MWCNTs is challenging because of dispersion of the MWCNTs in the polymer matrix, as documented in Figures 4 to 6.

Conclusions

We have demonstrated a method to concentrate and align MWCNTs within polymer nanocomposite materials using ultrasound directed self-assembly. The novelty of this work is that we achieve an ultra-high weight fraction of aligned MWCNTs (>10 wt.%) by introducing a small weight fraction (1.0 wt.%) of MWCNTs to the polymer matrix, enabling uniform dispersion of the MWCNTs, and then employing ultrasound directed self-assembly to concentrate and align the MWCNTs along a single line to produce a polymer nanocomposite material with locally ultra-high MWCNT weight fraction. Mechanical testing shows that this ultra-high weight fraction of aligned MWCNTs results in superior ultimate tensile strength, Young's modulus, and moduli of resilience and toughness, compared to benchmark materials containing lower weight fractions of aligned or randomly oriented MWCNTs, as well as virgin polymer matrix material. Additionally, the size of the error bars of the mechanical property measurements demonstrates repeatability of the manufacturing process. Thus, this method could be a promising new avenue to achieve synthesis and processing of polymer nanocomposite materials with ultra-high weight fraction of CNTs.

Acknowledgements

We thank Prof. Daniel O. Adams for access to mechanical testing infrastructure in the Structural Integrity Laboratory at the University of Utah – Department of Mechanical Engineering.

Declaration of Conflicting Interests

The author(s) declared no potential conflicts of interest with respect to the research, authorship, and/or publication of this article.

Funding

The author(s) disclosed receipt of the following financial support for the research, authorship, and/or publication of this article: JG and BR acknowledge support from Army Research Office contract# W911NF-16-1-0457. JG also acknowledges partial support of a National Aeronautics and Space Agency Space Technology Research Fellowship (award# NNX15AP30H).

ORCID iD

B Raeymaekers  <http://orcid.org/0000-0001-5902-3782>

References

1. Moniruzzaman M and Winey KI. Polymer nanocomposites containing carbon nanotubes. *Macromolecules* 2006; 39: 5194–5205.

2. Du J-H. The present status and key problems of carbon nanotube based polymer composites. *EXPRESS Polym Lett* 2007; 1: 253–273.
3. Haslam MD and Raeymaekers B. A composite index to quantify dispersion of carbon nanotubes in polymer-based composite materials. *Compos Part B* 2013; 55: 16–21.
4. Schadler LS, Giannaris SC and Ajayan PM. Load transfer in carbon nanotube epoxy composites. *Appl Phys Lett* 1998; 73: 3842–3844.
5. Greil P. Perspectives of nano-carbon based engineering materials. *Adv Eng Mater* 2015; 17: 124–137.
6. Le MT and Huang S-H. Effect of nano-fillers on the strength reinforcement of novel hybrid polymer nanocomposites. *Mater Manuf Proc* 2016; 31: 1066–1072.
7. Coleman JN, Khan U, Blau WJ, et al. Small but strong: a review of the mechanical properties of carbon nanotube-polymer composites. *Carbon* 2006; 44: 1624–1652.
8. Li YL, Kinloch IA and Windle AH. Direct spinning of carbon nanotube fibers from chemical vapor deposition synthesis. *Science* 2004; 304: 276–278.
9. Wang W, Yong ZZ, Li QW, et al. Ultrastrong, stiff and multifunctional carbon nanotube composites. *Mater Res Lett* 2013; 1: 19–25.
10. Jin L, Bower C and Zhou O. Alignment of carbon nanotubes in a polymer matrix by mechanical stretching. *Appl Phys Lett* 1998; 73: 1197.
11. Ajayan PM, Stephan O, Colliex C, et al. Aligned carbon nanotube arrays formed by cutting a polymer resin-nanotube composite. *Science* 1994; 265: 1212–1214.
12. Fan Z and Advani SG. Characterization of orientation state of carbon nanotubes in shear flow. *Polymer* 2005; 46: 5232–5240.
13. Chen XQ, Saito T, Yamada H, et al. Aligning single-wall carbon nanotubes with an alternating-current electric field. *Appl Phys Lett* 2001; 78: 3714.
14. Kamat PV, Thomas KG, Barazzouk S, et al. Self-assembled linear bundles of single wall carbon nanotubes and their alignment and deposition as a film in a dc field. *J Am Chem Soc* 2004; 126: 10757–10762.
15. Fujiwara M, Oki E, Hamada M, et al. Magnetic orientation and magnetic properties of a single carbon nanotube. *J Phys Chem A* 2001; 105: 4383–4386.
16. Strobl CJ, Schäflein C, Beierlein U, et al. Carbon nanotube alignment by surface acoustic waves. *Appl Phys Lett* 2004; 85: 1427–1429.
17. Haslam MD and Raeymaekers B. Aligning carbon nanotubes using bulk acoustic waves to reinforce polymer composites. *Compos Part B* 2014; 60: 91–97.
18. Lim WP, Yao K and Chen Y. Alignment of carbon nanotubes by acoustic manipulation in a fluidic medium. *J Phys Chem C* 2007; 111: 16802–16807.
19. De Heer WA. Nanotubes and the pursuit of applications. *Mater Res Soc Bull* 2004; 29: 281–285.
20. Gor'kov LP. On the forces acting on a small particle in an acoustical field in an ideal fluid. *Soviet Doklady Phys* 1962; 6: 773.
21. Landau LD and Lifshitz EM. *Fluid mechanics*. Oxford: Pergamon Press, 1987.
22. Saito M, Daian T, Hayashi K, et al. Fabrication of a polymer composite with periodic structure by the use of ultrasonic waves. *J Appl Phys* 1998; 83: 3490.
23. Scholz M-S, Drinkwater BW and Trask RS. Ultrasonic assembly of anisotropic short fibre reinforced composites. *Ultrasonics* 2014; 54: 1015–1019.
24. Pötschke P, Fornes TD and Paul DR. Rheological behavior of multiwalled carbon nanotube/polycarbonate composites. *Polymer* 2002; 43: 3247–3255.
25. Greenhall J, Guevara Vasquez F and Raeymaekers B. Continuous and unconstrained manipulation of micro-particles using phase-control of bulk acoustic waves. *Appl Phys Lett* 2013; 103: 074103.
26. Raeymaekers B, Pantea C and Sinha DN. Manipulation of diamond nanoparticles using bulk acoustic waves. *J Appl Phys* 2011; 109: 014317.
27. Greenhall J, Guevara Vasquez F and Raeymaekers B. Ultrasound directed self-assembly of user-specified patterns of nanoparticles dispersed in a fluid medium. *Appl Phys Lett* 2016; 108: 103103.
28. Doinikov AA. Acoustic radiation force on a spherical particle in a viscous heat-conducting fluid. II. Force on a rigid sphere. *J Acoust Soc Am* 1997; 101: 722–730.
29. Collino RR, Ray TR, Fleming RC, et al. Acoustic field controlled patterning and assembly of anisotropic particles. *Extreme Mech Lett* 2015; 5: 37–46.
30. ASTM Standard D638-14. *Standard test method for tensile properties of plastics*. West Conshohocken, PA: ASTM International, 2013.
31. Smooth-On, Inc. 2015. *Smooth-Cast 300 Series*, www.smooth-on.com/tb/files/Smooth-Cast_300q_300_-305_310.pdf (accessed 6 September 2018).
32. Islam MF, Rojas E, Bergey DM, et al. High weight fraction surfactant solubilization of single-wall carbon nanotubes in water. *Nano Lett* 2003; 3: 269–273.
33. Mensah B, Kim HG, Lee JH, et al. Carbon nanotube-reinforced elastomeric nanocomposites: a review. *Int J Smart Nano Mater* 2016; 6: 211–238.
34. Huang YY and Terentjev EM. Dispersion of carbon nanotubes: mixing, sonication, stabilization, and composite properties. *Polymers* 2012; 4: 275–295.
35. Cheap Tubes, Inc. 2016. *Multi Walled Carbon Nanotubes*, www.cheaptubes.com/product/multi-walled-carbon-nanotubes-50nm/ (accessed 6 September 2018).